Molecular Neurobiology (2019) 56:3368–3379
https://doi.org/10.1007/s12035-018-1312-5

Degradation of Caytaxin Causes Learning and Memory Deficits via Activation of DAPK1 in Aging

Yu Guo[1,2] · Hao Li[1,2] · Xiao Ke[1,2] · Manfei Deng[1,2] · Zhuoze Wu[1,2] · You Cai[1,2] · Henok Kessete Afewerky[2,3] · Xiaoan Zhang[1,2] · Lei Pei[2,4] · Youming Lu[1,2]

Received: 1 May 2018 / Accepted: 8 August 2018 / Published online: 17 August 2018

Abstract

Loss of memory is an inevitable clinic sign in aging, but its underlying mechanisms remain unclear. Here we show that death-associated protein kinase (DAPK1) is involved in the decays of learning and memory in aging via degradation of Caytaxin, a brain-specific member of BNIP-2. DAPK1 becomes activated in the hippocampus of mice during aging. Activation of DAPK1 is closely associated with degradation of Caytaxin protein. Silencing Caytaxin by the expression of small interfering RNA (siRNA) that targets specifically to Caytaxin in the hippocampus of adult mice impairs the learning and memory. Genetic inactivation of DAPK1 by deletion of DAPK1 kinase domain prevents the degradation of Caytaxin and protects against learning and memory declines. Thus, activation of DAPK1 impairs learning and memory by degrading Caytaxin during aging.

Keywords DAPK1 · Caytaxin · Aging · Learning and memory

Introduction

Senescence refers to a process whereby organisms become physiologically and psychologically less efficient at adapting to their environment and gradually advent toward death [1]. Senescence can be divided into two types, namely physiological senescence and pathological senescence [2]. The former is a physiological degeneration after maturity, whereas the latter results from external factors such as various diseases. In the process of physiological senescence, a series of behavioral changes emerge, including sleeping disorder, cognitive deficit, and social dysfunction [3–8]. In this type of senescence, learning and memory deficit is a significant sign of brain aging. But both the cellular and molecular mechanisms underlying age-dependent decays of learning and memory remain unclear.

Caytaxin, first discovered by Bomar [9] in Cayman ataxia, is a protein encoded by Atcay/ATCAY gene. In line with the system of protein nomenclature, abnormal gene products of ataxia are termed as ataxins [10]. Cayman ataxia is an autosomal recessive hereditary disease, with a feature of mental retardation and obvious bradykinesia [11]. The first published analysis of Atcay/ATCAY mRNA location in mice predicted stable expression of Caytaxin exclusively in the nervous system [12]. This was verified via in situ hybridizations of mouse brain and embryo, whereby most brain regions including the cortex, hippocampus, cerebellum, and olfactory bulb showed abundant expression of Caytaxin [12]. Moreover, in mouse embryo, Atcay was detected in some regions of the nervous system, such as trigeminal nerve, butterfly pupa, and dorsal root ganglia [12]. Highly specific position and high abundant expression of Atcay/ATCAY mRNA indicate that Caytaxin may play a fundamental role in the nervous system. And studies have demonstrated that Caytaxin is expressed in presynaptic granule cells [12], involved in synaptic transmission

Yu Guo and Hao Li contributed equally to this work.

✉ Lei Pei
peilei@hust.edu.cn

✉ Youming Lu
lym@hust.edu.cn

[1] Department of Physiology, School of Basic Medicine and Tongji Medical College, Huazhong University of Science and Technology, Wuhan 4030030, China

[2] The Institute for Brain Research, Collaborative Innovation Center for Brain Science, Huazhong University of Science and Technology, Wuhan 430030, China

[3] Department of Pathology and Pathophysiology, School of Basic Medicine and Tongji Medical College, Huazhong University of Science and Technology, Wuhan 430030, China

[4] Department of Neurobiology, School of Basic Medicine and Tongji Medical College, Huazhong University of Science and Technology, Wuhan 4030030, China

through highly conservative protein structure. Accordingly, a decreased expression of Caytaxin caused by Atcay/ATCAY mutation may explain the motility, physical, and cognitive deficits in animals that carried the mutant gene [9].

Several proteins have been reported to be associated with Caytaxin in the central neurons. One of them is death-associated protein kinase (DAPK1), which is a serine/threonine protein kinase, consisting of a kinase domain, a calmodulin (CaM)-binding motif, eight repeats of anchored proteins, and a death domain. CaM-binding motif contains binding sites and self-inhibition area [13]. A bind of DAPK1 to the CaM-binding site results to DAPK1 conformational changes, reactivation of CaM-blocked active sites and DAPK1 activation [13, 14]. Previous studies show that activated DAPK1 is involved in some apoptosis-mediated cell death, including apoptosis modulated by Fas [15], tumor necrosis factor [15], apoptotic protease [16], and p53 [17]. DAPK1 is associated with nerve injury-related neurological diseases and accordingly has been target for the treatment of stroke, epilepsy, and Alzheimer's disease. Recently, we reported that DAPK1 activation is involved in the impairments of synaptic transmission and spatial learning and memory. Both DAPK1 and Caytaxin proteins are physically associated and highly expressed in the hippocampus. Thus, it is probably that the reduction of Caytaxin protein expression is mediated by activation of DAPK1 in aging.

In this study, we observed that Caytaxin proteins, but not mRNA levels in the hippocampus of aged mice were dramatically reduced, as compared to young adult mice. The reduction of Caytaxin protein expression correlated with the increase of the enzymatic activity of DAPK1. Genetic inactivation of DAPK1 inhibited Caytaxin degradation and improved spatial learning and memory in aging.

Methods

Antibodies and Chemicals

We used the following antibodies and chemicals: anti-cleaved caspase3 antibody (Cell Signaling, #9664); anti-Caytaxin antibody (Santa Cruz Biotechnology, sc-65018); anti-DAPK1 antibody (Cell Signaling, #3008); anti-DAPK1-N terminal antibody (Sigma, SAB1304437); anti-DAPK1-C terminal antibody (OriGene, TA324907); anti-pMLC antibody (Cell Signaling, #3671); anti-β-actin antibody (Proteintech Group, 66009-1-lg); anti-FLAG antibody (Cell Signaling, #2368); anti-$p16^{INK4A}$ antibody (Proteintech Group, 10,883-AP); anti-p53 antibody (Millipore, MABE283); HS38(Sigma, SML0929); z-VAD-fmk (Bachem, N-1510); D-(+)-galactose (Sigma, G0750).

Animals

All mice used in this study were bred and reared in the same conditions in accordance with institutional guidelines of the Animal Care and Use Committee (Huazhong University of Science and Technology, Wuhan, China) within the University' s animal care facility. Mice were housed in groups of three to five per cage under a 12-h light-dark cycle, with lights on at 8 a.m., at a consistent ambient temperature (21 ± 1 °C) and humidity (50 ± 5%). In the present study, only male mice were used to avoid behavioral variability between genders. All experiments and analyses were performed blind to the mice genotype or treatment.

Generation of the Genetic Mutant Mice

To identify the specific impacts of kinase domain of DAPK1 in aged brain, we generated a conditional mutant strain of mice with a selective deletion of kinase domain of DAPK1 in brain (DAPK1-$KD^{-/-}$ mice) by crossing DAPK1-$KD^{loxp/loxp}$ transgenic mice with CaMK2α-creERT2 mice (stock number: 012362, The Jackson Laboratory, Bar Harbor, ME, USA). The mutant mice were treated with tamoxifen (Tam) dissolved in corn oil (100 mg/kg, *i.p.*, once per day for 5 consecutive days).

Generation of the Lentivirus Particles

Atcay (NM_178662.3) was cloned into the FUGW2.1 construct containing eGFP through *Bam*HI/*Age*I (New England Biolabs). The Atcay plasmids were co-transfected with CMV and ΔR8.91 into HEK293ft cells to generate the lentivirus particles.

Stereotaxic Injection

Mice (C57BL/6 10 weeks, male) were anesthetized with isoflurane (2–5%) and placed in a stereotaxic apparatus. The head was fixed and the skull was exposed. Burr holes were made and a micro-syringe (World Precision Instruments) was slowly lowered into the dorsal DG at 2.06 mm anteroposterior, 1.38 mm mediolateral, and 2.10 mm dorsoventral relative to bregma. For the mouse line validation, for the electrophysiological and behavior experiments, 1 μL of virus was pressure-injected into each hemisphere. After injection, the needle remained in place for 5 min and was then slowly retracted to avoid leakage. The mice were placed on a heating pad throughout the duration of the surgery. After injection, the scalp was sutured. The mice were placed on the heating pad during recovery from anesthesia. The electrophysiological and behavior experiments were proceeded 4 weeks after the virus injection.

Western Blot

Cells were rinsed twice in PBS at pH 7.5 and lysed with buffer containing 50 mM Tris-HCl, pH 8.0, 150 mM NaCl, 1% NP-40, 0.5% sodium deoxycholate, 0.1% SDS, 0.02% NaN_3, 100 mg/mL PMSF, and 10 mg/mL each of the protease inhibitors (leupeptin, aprotinin, and pepstatin A). Cell lysates were then centrifuged at 12,000*g* for 5 min at 4 °C; aliquots of supernatants were added to one-third volume of 4× sample buffer, followed by boiling for 10 min and then sonication for 5 s on ice. Protein concentration was quantitated using the BCA Protein Assay Reagent (Pierce). The hippocampi were isolated from the mice brain and homogenized in buffer as cells, and then were added to one-third volume of 4× sample buffer and boiled for 10 min in a water bath. Protein concentration was quantitated using the BCA Protein Assay Reagent (Pierce).

The proteins prepared were separated by 10% sodium dodecyl sulfate-polyacrylamide gels (SDS/PAGE) and then transferred onto nitrocellulose filter membrane (NC). After being blocked with blocking solution (5% nonfat dried milk diluted with Tris-buffered saline containing 0.1% Tween-20, TBST buffer, pH 7.5) for 1 h at room temperature, the transfer membranes were incubated with primary antibody diluted with 3% bovine serum albumin (BSA) in TBST buffer overnight at 4 °C. On the second day, membranes were first washed with TBST for 10 min × 4 times, then membranes were incubated with respective secondary antibodies for 1 h at room temperature, and then the protein signals were scanned using an Infrared Imaging System (Odyssey, LI-COR).

Open Field

Locomotor activity was measured in clear boxes measuring 43.2 cm × 43.2 cm, outfitted with photo-beam detectors for monitoring horizontal and vertical activities, as described before. Data were collected via a PC and were analyzed with the MED Associates' Activity Monitor Data Analysis software. Mice were placed in a corner of the open-field apparatus and left to move freely. Recorded variables include the following: resting time (s), ambulatory time (s), vertical/rearing time (s), jump time (s), stereotypic time (s), and average velocity (cm/s). Mice were not exposed to the chamber before testing. Data were individually recorded for each animal during 30 min.

Elevated Plus Maze

The plus maze had two walled arms (the closed arms, 35 cm L × 6 cm W × 22 cm H) and two open arms (35 cm L × 6 cm W). The maze was elevated 74 cm from the floor. Mice were placed on the center section and allowed to explore the maze freely and monitored with ImageEP software66. Time spent in the open versus closed arms during the 10-min period was presented.

Morris Water Maze

The water maze task consists a circular tank (120 cm diameter) filled with opaque water (21–23 °C) and a hidden platform (6 cm diameter) submerged 1 cm below the surface of the water, as described before. Device with software [WMT-100] was purchased from Tai Meng Technology Co., Ltd. (Chengdu, China). Before the start of training trials, the mice were allowed to acclimate to testing room for 30 min. The mice were trained to find the invisible platform within 90 s on 6 consecutive days with three trials per day. Mice that failed to find the platform within 90 s were guided to find the platform and allowed to remain there for 15 s. Escape latency to find the hidden platform, path length, and swimming velocity was recorded. After 1 day of rest, the platform was removed and mice were individually set afloat to search the poor for 90 s (probe tests). Then, the time spent in each quadrant was analyzed.

Fear Conditioning Tests

The experimental device and recording software [FCT-100] were purchased from Tai Meng Technology Co., Ltd. (Chengdu, China). Before training, the mice were placed into a lonely chamber (33 × 33 × 35 cm^3) with a metal grid at the bottom for 5 min to adapt the novel environment and the numbers and percentages of freezing behavior were recorded. On the training day, the mice were given 5-min trials that began with a 30-s tone, followed by a 2-s foot-shock (1 mA) and then a 30-s interval, repeated three times. After 24 h, contextual and tone conditioning tasks were assessed. To test contextual conditioning fear, mice were returned to the same chamber and contextual learning was assessed following the same procedure as in the training day except for the foot-shock and tone. To test tone-dependent conditioning fear, the environment in the chamber was changed (visual, tactile, and olfactory cues) to present mice with a new context for testing. Then mice were placed in the chamber for 5 min and the same assessment procedure was followed as in the training day except for the foot-shock.

Reverse Transcription and Quantitative PCR

The cDNA synthesis kit (TOYOBO) was used for the reverse transcription reaction according to the manufacturer's instructions. We used 1 μg total RNA. Samples were incubated for 5 min at 65 °C. All samples were then added to a 5× mix, heated to 37 °C for 15 min, and reactions were stopped by heating to 98 °C for 5 min. For quantitative PCR (qPCR), all specific primers were selected using Beacon Designer

Software (BioRad) and synthesized by Tsingke (Wuhan, China). The PCR amplification of each product was further assessed using fivefold dilutions of mouse brain cDNA library as a template and found to be linear over five orders of magnitude and at greater than 95% efficiency. The reactions were set up in duplicate in total volumes of 10 μL containing 5 μL 2× miScript SYBR green PCR kit (Genecopoeia) and 2 μL template (1:5 dilution from RT product) with a final concentration of 400 nM of the primer. The PCR cycle was as follows: 95 °C/3 min, 40 cycles of 95 °C/30 s, 60 °C/45 s, and 95 °C/1 min, and the melt-curve analysis was performed at the end of each experiment to verify that a single product per primer pair was amplified. The amplification and analysis were performed using an iCycleriQ Multicolor Real-Time PCR Detection System (BioRad). Samples were compared using the relative CT method. The fold increase or decrease was determined relative to a vehicle-treated control after normalizing to a housekeeping gene using 2-ΔΔCT, where the ACT is (gene of interest CT) − (GAPDH CT), and ΔΔCT is (ΔCT treated) − (ΔCT control). The following primers (5′ to 3′) were used: DAPK1 forward, CAGGAGCGTCTGGG TCTAAG, and DAPK1 reverse, CCGTGCTGTGTAGC TGTTGT; DAPK1-KD forward, CAAATGTCATCACCCT-GCAT, and DAPK1 reverse, GTTGCCTCCTCTTC AGTCAGA; Caytaxin forward, AATGGCAGGATGAG GATCTG, and Caytaxin reverse, CAGTTTCATCTGGC GTC-TCA. The results were computed using a standard curve made with cDNA pooled from all samples.

Electrophysiological Recordings In Vitro

Slice preparation: the slices (350 μm) of the hippocampus were cut from 120 days male mice and were placed at 28–32 °C holding chamber for at least 1 h. A single slice was then transferred to the recording chamber and then submerged and perfused with artificial CSF (ACSF, 2 mL/min) that had been saturated with 95% O_2 and 5% CO_2. The composition of the ACSF was (1 L): 124.0 g NaCl, 3.0 g KCl, 1.25 g NaH_2PO_4, 2.0 g $MgCl_2$, 2.0 g $CaCl_2$, 3.0 g $NaHCO_3$, and 10 g glucose. We used standard procedures to record field excitatory postsynaptic potentials (fEPSPs) in the CA1 region of the hippocampus. A bipolar stimulating electrode (FHC Inc., Bowdoin, ME) was placed in the Schaffer collaterals to deliver test and conditioning stimuli. A borosilicate glass recording electrode filled with ACSF was positioned in stratum radiatum of CA1, 200–300 mm from the stimulating electrode. fEPSP in the CA1 region were induced by test stimuli at 0.1 Hz with an intensity that elicited a fEPSP amplitude 35% maximum. Test responses were recorded for 30–60 min prior to beginning the experiment to assure the stability of the response. Once a stable test response was attained, a baseline was recorded for an additional 30 min. To induce LTP, three consecutive trains (500 ms) of stimuli at 100 Hz separated by 10 s were applied to the slices, a protocol that induced LTP lasting approximately 1 h different genetic background mice. The field potentials were amplified 100× using an Axon Instruments 200B amplifier and digitized with Digital data 1440A. Data were sampled at 10 kHz and filtered at 2 kHz. Traces were obtained by pClamp 9.0 and analyzed using the pClampfit 9.0. LTP values reported throughout the course were measured at 60 min after the conditioning stimulus.

A whole-cell recording (tight seal, > 10 GΩ) with patch electrode (3–5 MΩ) was obtained from the Caytaxin$^+$ and Caytaxin$^-$ granule neurons, respectively. The miniature EPSCs (mEPSCs) were recorded in the presence of 1 mM tetrodotoxin and 100 mM bicuculline at the holding potential of − 70 mV.

Primary Neuron Culture

Hippocampi were isolated from the E18 C57BL/6 mice, as we described before. Cells were platted with the densities of 100–150 cells/mm^2 on plates coated with 0.1 mg/mL poly-D-lysine. Cells were homogenized in fresh serum-free neurobasal medium (21103, GIBCO) plus 2% B27 and were fed every 3 days with fresh media. The neuronal cultures were treated with lentivirus at 9 days DIV, then tested after 1 week. To establish a senescent cell model, the neuronal cultures were treated with D-galactose at 6 days DIV and consecutive 3 days. To detect whether the aging model is successful, p16 and p53 in the lysates were blotted with anti-p16 (1:1000; PTG) and anti-p53 (1:1000; Millipore).

Statistical Analysis

All values in the text and figure legends are represented as the mean ± SEM. Parametric tests, including *t* tests and two-way ANOVAs, were used when assumptions of normality and equal variance (*F* test) were met; two-way repeated measures ANOVA was used to analyze the Morris water maze data. Statistical analyses were performed using Graph Prism 6. Statistically significant differences were defined as $p < 0.05$.

Results

A Reduction of Caytaxin Protein Correlates with DAPK1 Activation in Aging Process

To detect brain senescence, we analyzed aging-related proteins p53 and p16 in the hippocampus tissue of 4, 8, 12, and 18 months old mice brain (Fig. 1a). Our data showed that the protein levels of p53 and p16 were increased with aging and peaked at 18 months (Fig. 1b). To identify the molecular mechanism underlying the aging-related impairments of the synapse in hippocampal mossy fibers, we focused on DAPK1, a serine- and threonine-dependent calmodulin kinase, which is

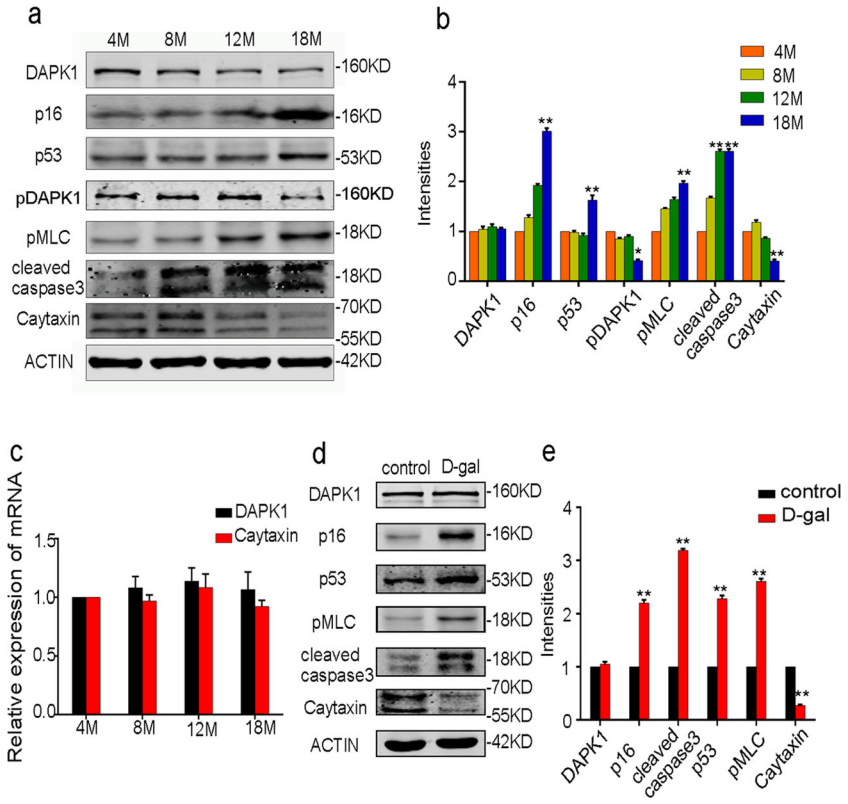

Fig. 1 A reduction of Caytaxin protein correlates with DAPK1 activation in aging. **a** Representatives of western blots in cell lysates from the hippocampus in different age groups. **b** Bar graphs show the band intensities that were normalized to β-actin from mice at 4 months (defined as 1.0). Data are mean ± SEM ($n = 6$ mice per group, $^{**}p < 0.01$, compared to the respective group at 4 months old of age, *t* tests). **c** Bar graphs show the relative expression of mRNA in different age groups of DAPK1 and Caytaxin. Data are mean ± SEM ($n = 6$ mice per group, compared to the respective group at 4 months old of age). **d** Representatives of western blots in cell lysates from primary cultured neurons treated with D-galactose. **e** Bar graph shows the band intensities that were normalized to the respective control (defined as 1.0). Data are mean ± SEM ($n = 6$ assays, $^{**}p < 0.01$, compared to the respective controls, *t* tests)

closely associated with synaptic injury. To determine the activity of DAPK1, we detected the phosphorylation of DAPK1 (pDAPK1) and phosphorylation of MLC (pMLC) which is the endogenous substrate of DAPK1. Our data showed that the protein level of pDAPK1 was gradually decreased, while pMLC was increased with age in the hippocampus (Fig. 1a, b). Additionally, our data also showed a similar increase pattern of cleaved caspase3 with p16 and pMLC (Fig. 1a, b). As regards Caytaxin, it was increased and peaked at 8 months and then decreased to the lowest level at 18 months (Fig. 1a, b), while the protein level of DAPK1 showed no significant change in all groups of mice from 4 to 18 months (Fig. 1a, b). Then we established an in vitro aging model with primary hippocampal neurons by using D-galactose (D-GAL) [18]. Our data showed the consistent results with the in vivo studies of aged mice. The levels of p53, p16, pMLC, and cleaved caspase3 were elevated, while the level of Caytaxin was reduced after treatment with D-GAL (Fig. 1d, e). Therefore, the reduction of Caytaxin is parallel with the activation of DAPK1 and caspase3 during aging, which indicates that loss of Caytaxin protein may correlate with DAPK1 activation in aging process.

Silencing Caytaxin Reduces Neuronal Excitability and Impairs Learning and Memory

To explore the role of Caytaxin in neurons, we transfected primary cultured hippocampal neurons at day 9 with Lenti-Virus-Caytaxin-EGFP (LV-cay), Lenti-Virus-si-Caytaxin-EGFP (LV-si-cay), and the control Lenti-Virus-EGFP (LV-NC) (Fig. 2a). Successful transfections of Caytaxin or si-Caytaxin were confirmed by western blot experiments 28 days after the above lentivirus transfections (Fig. 2b). We recorded AMPA receptor-mediated component of mini-EPSCs (mEPSCs) in the presence of 10 μM bicuculline at the holding potential of − 70 mV. Our data showed a significant decline in both amplitude and frequency of mEPSCs in the neurons transfected with LV-si-cay but conversely increased in neurons transfected with LV-cay (Fig. 2c, d).

To further investigate the role of Caytaxin in neuronal excitability and the ability of learning and memory, we injected LV-cay, LV-si-cay, and LV-NC respectively into the hilus of DG area in three independent groups of 3 months old mice (Fig. 2e). Successful transfections of Caytaxin or si-Caytaxin were confirmed by western blot experiments 28 days after the

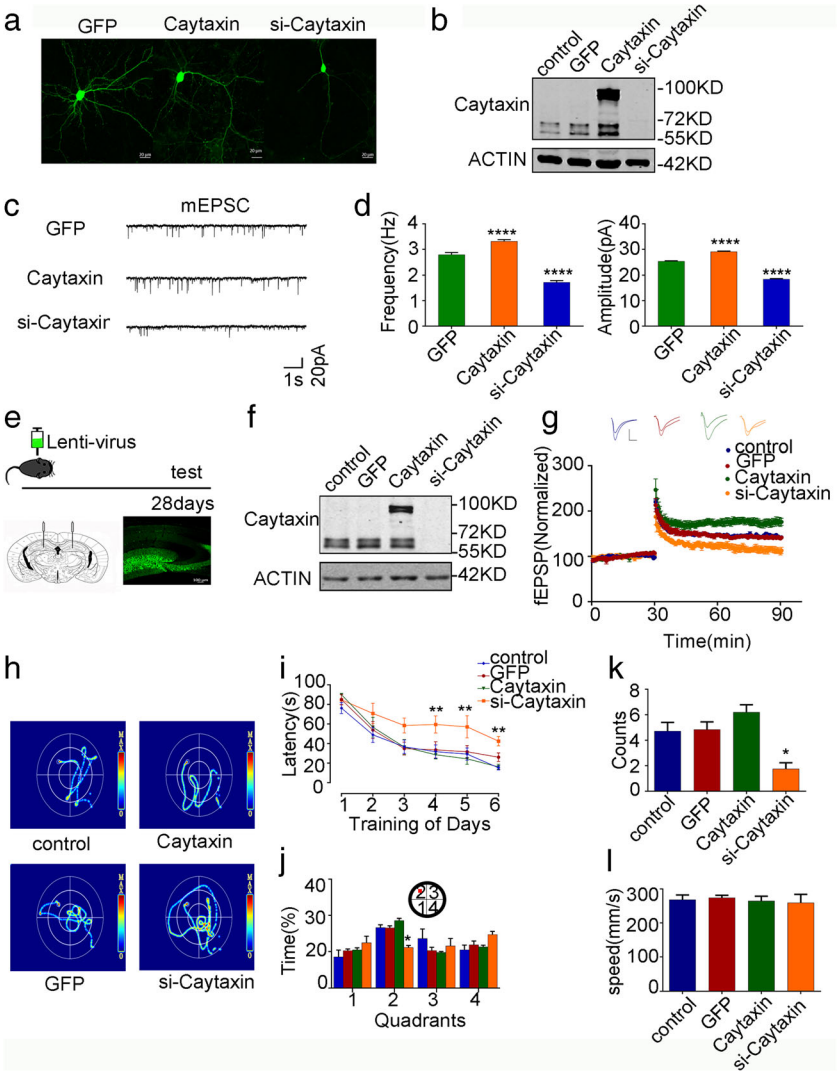

Fig. 2 Silencing Caytaxin reduces neuronal excitability and impairs learning and memory. **a** Representatives of images show the expression of GFP control, Caytaxin, and si-Caytaxin in primary cultured neurons (DIV15) using lentivirus vectors (LV-FUGW2.1-CMV-GFP versus LV-FUGW2.1-CMV-Caytaxin-GFP and LV-FUGW2.1-CMV-si-Caytaxin-GFP). **b** Western blots in cell lysates from primary cultured neurons with the expression of GFP or Caytaxin or si-Caytaxin or without the expression of virus (control). **c** Representatives of recordings show the miniature EPSCs (mEPSCs) from primary cultured neurons with the expression of GFP, Caytaxin, and si-Caytaxin. **d** Bar graphs show the frequencies and the mean amplitudes of mEPSCs, respectively. Data are mean ± SEM ($n = 21$ recordings/group, $^{****}p < 0.0001$, compared to the GFP group). **e** Illustration shows the experimental schedules of LV-GFP or LV-Caytaxin or LV-si-Caytaxin. Mice were injected with lentivirus vectors (LV-FUGW2.1-CMV-GFP versus LV-FUGW2.1-CMV-Caytaxin-GFP and LV-FUGW2.1-CMV-si-Caytaxin-GFP) in the hippocampus of adult mice. **f** Representatives show western blots in cell lysates from the hippocampus, the expression of GFP or Caytaxin or si-Caytaxin, or without the expression of virus (control). **g** The representative recordings (top) and the normalized slope (bottom) of the fEPSPs. Data are mean ± SEM ($n = 12$ recordings/6 mice/group). **h**–**l** The behaviors of mice injected with LV-GFP or LV-Caytaxin or LV-si-Caytaxin were examined. **i** The average latency to reach a hidden platform is plotted against the blocks of trials (days) in Morris water maze tests. Data are reported as the mean ± SEM ($n = 10$ mice per group, $^{**}p < 0.01$, compare to the control group). **j** The percentage of time spent in searching of a hidden platform in each quadrant during the probe trial. Data are reported as the mean ± SEM ($n = 10$ mice per group, $^{*}p < 0.05$, compare to the control group). **k** Bar graph shows the times of crossing the place of the hidden platform during the probe trial. Data are reported as the mean ± SEM ($n = 10$ mice per group, $^{*}p < 0.05$, compare to the control group). **l** Bar graph shows the swimming speed of mice during the probe trial. Data are reported as the mean ± SEM ($n = 10$ mice per group)

above lentivirus injections (Fig. 2f). Then we recorded fEPSPs in the CA1 region by electrical stimulation of the mossy fiber tracks that reflect synaptic responses from neurons in the dentate gyrus. In comparison to the control group, our results demonstrate that silencing Caytaxin impairs LTP, while on the contrary, over-expression of Caytaxin improves LTP ($n = 12$ recordings/6 mice, Fig. 2g).

We next analyzed the mice behavioral performance and found that treatment with LV-NC, LV-si-cay, and LV-cay does not affect locomotion. However, after LV-si-cay treatment, we

observed worse performance of the mice in Morris water maze tests than the other groups (Fig. 2h). Specifically, LV-si-cay-treated mice showed longer latency to reach the hidden platform during the training session and spent longer percentage time in search of the hidden platform in each quadrant during the probe trial than the other groups (42.46 ± 4.84 s (latency), and 22.25 ± 1.14 (percentage time) in mice after treatment with LV-si-cay versus 15.19 ± 2.27 s (latency), and 33.27 ± 1.53 (percentage time) in control mice; and 26.07 ± 4.36 s (latency), and 33.12 ± 1.10 (percentage time) in mice after treatment with LV-NC and 16.15 ± 2.56 s (latency), and 37.20 ± 1.15 (percentage time) in mice after treatment with LV-cay, mean ± SEM, $n = 10$ mice/group, Fig. 2i–l). These findings indicate that silencing Caytaxin decreases the neuronal excitability and accordingly damages spatial learning and memory.

Activation of DAPK1 Degrades Caytaxin via Caspase3

It has been elucidated that Caytaxin can be degraded by caspase3, which is activated via DAPK1. To test whether the degradation of Caytaxin is mediated by DAPK1 during aging, firstly, an in vitro model of aging was established by induction of D-galactose to primary cultured neurons. We used different concentrations of D-galactose (0, 4, 40, 400 mM) (Fig. 3a, b), out of which the cultured primary hippocampal neurons treated with 40 mM D-galactose consecutively for 3 days were the best strategy, considering the neuronal toxicity of D-galactose. Secondly, we treated the neuronal cells with HS38 (10 μM) [19] for inhibition of DAPK1 and z-VAD-fmk (1 μM) [20] for inactivation of caspase3 respectively. Interestingly, we noted that inhibition of DAPK1 or caspase3 could reduce the degradation of Caytaxin (Fig. 3c, d). Then, in order to determine whether the activation of caspase3 lies on DAPK1 activity dependent, the plasmids of DAPK1K42A (inactivated DAPK1), DAPK1ΔCaM (activated DAPK1), or the vector were transfected into HEK293T cells. We found that DAPK1ΔCaM increased the levels of cleaved caspase3. In addition, the degradation of Caytaxin was also increased in DAPK1ΔCaM, but not DAPK1K42A-transfected HEK293T cells (Fig. 3e, f). These data demonstrate that the activated DAPK1 partly degrades Caytaxin by the activation of caspase3.

Inactivation of DAPK1 Inhibits Caytaxin Degradation in Aging

It is known that activation of DAPK1 degrades Caytaxin via caspase3; next we investigated whether inactivation of DAPK1 in the hippocampus of aged mice inhibits the degradation of Caytaxin. Then, we generated a mutant strain of mice (DAPK1-KD^{loxploxp}) in which a double-floxed inversely open reading frame of DAPK1 with a kinase domain deletion was expressed. When these mice were bred with CaMK2α-creERT2 mice, containing Cre recombinants expressed in excitatory neurons, the kinase domain of DAPK1 was selectively deleted in excitatory neurons of the offspring after induction of tamoxifen (Fig. 4a). RT-PCR and western blot analysis revealed successful deletion of the kinase domain of DAPK1 mRNA and proteins in the hippocampus of DAPK1-KD$^{-/-}$ mice (Fig. 4d, e). Furthermore, conditional knockout of the kinase domain of DAPK1 has no influence on the animals' general phenotype, such as body weight gain (Fig. 4c), brain structure (Fig. 4b), and anxiety-like behavior (Fig. 4f). These results confirm the successful deletion of kinase domain of DAPK1 in the brain, and this deletion does not alter any phenotype in mice.

To investigate whether the genetic inhibition of DAPK1 might avert the degradation of Caytaxin during aging, we compared the protein levels of cleaved caspase3, p53, and p16 in the hippocampus of 4 and 18 months old DAPK1KD$^{loxp/loxp}$ and DAPK1-KD$^{-/-}$ mice. We found that the DAPK1-KD$^{-/-}$ aged mice showed less cleaved caspase3, p53, and p16, but more Caytaxin, than the DAPK1-KD$^{loxp/loxp}$ aged mice (Fig. 4g–i). Altogether, these data demonstrate that the inhibition of DAPK1 by selective deletion of DAPK1-KD in the hippocampus prevents the degradation of Caytaxin during aging.

Inhibition of Caytaxin Degradation Rescues Learning and Memory Deficits in Aging

We next investigated whether preventing the degradation of Caytaxin via the inhibition of DAPK1 in the hippocampus improves learning and memory in aged mice. To address this, we divided the mice into four groups as two groups of 4 months old DAPK1-KD$^{-/-}$ and DAPK1-KD$^{loxp/loxp}$ adult mice and other two groups of 18 months old DAPK1-KD$^{-/-}$ and DAPK1-KD$^{loxp/loxp}$ aged mice. We used standard procedures to record field excitatory postsynaptic potentials (fEPSPs) in the CA1 region of the hippocampus, and the induction of LTP was impaired in DAPK1-KD$^{loxp/loxp}$ aged mice, but not in DAPK1-KD$^{-/-}$ aged mice. Then, we analyzed the task performance of these mice in a hidden version of the Morris water maze test. Results showed no difference in swimming speed between wild-type and mutant mice in the same age group (Fig. 5f). Moreover, the latency to reach a hidden platform during the training session and the percentage of time spent in search of a hidden platform during the probe trial were comparable in all four groups: the DAPK1-KD$^{-/-}$ adult mice (23.14 ± 2.97 s (latency), 37.03 ± 1.67 (percentage time)); the DAPK1-KD$^{loxp/loxp}$ adult mice (23.45 ± 3.17 s (latency), 32.47 ± 1.03 (percentage time)); the DAPK1-KD$^{-/-}$ aged mice (25.08 ± 3.31 s (latency), 34.30 ± 1.22 (percentage time)); and the DAPK1-KD$^{loxp/loxp}$ aged mice (42.38 ± 4.81 s (latency), 23.22 ± 0.89 (percentage time)) (Fig. 5c, d). The adult groups showed no difference between DAPK1-KD$^{-/-}$

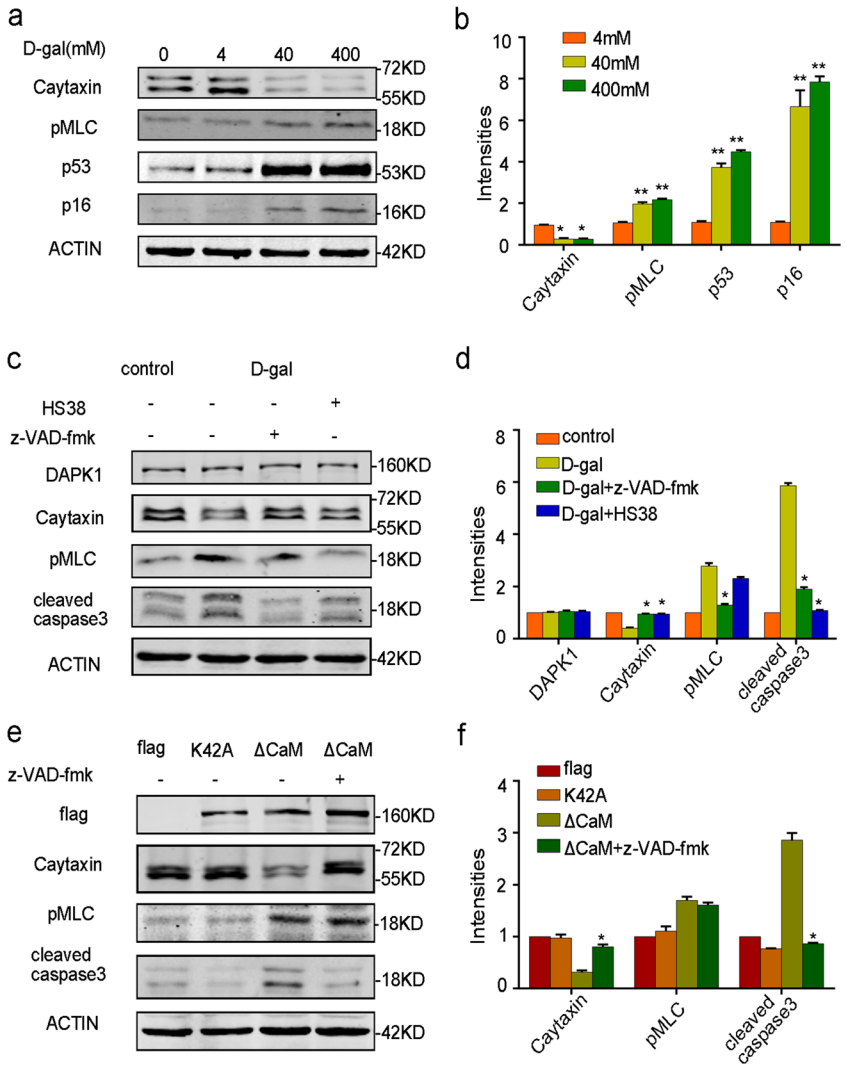

Fig. 3 DAPK1 degrades Caytaxin via activation of caspase3. **a** Representatives of western blots in cell lysates from primary neurons treated with D-gal at different concentrates. **b** Bar graphs show the band intensities that were normalized to the respective control (defined as 1.0). Data are mean ± SEM ($n = 6$ assays, $^{**}p < 0.01$, compared to the controls without D-galactose). **c** Representatives of western blots in cell lysates from primary neurons treated with HS38, z-VAD-fmk, and D-gal. **d** Bar graphs show the band intensities that were normalized to the respective control (defined as 1.0). Data are mean ± SEM ($n = 6$ assays, $^{*}p < 0.05$, compared to the group treated with D-gal). **e** Representatives of western blots in cell lysates from HEK293T cells transfected with the plasmid of Flag, DAPK1-K42A, DAPK1-ΔCaM, and DAPK1-ΔCaM with z-VAD-fmk. **f** Bar graphs show the band intensities that were normalized to the respective control (defined as 1.0). Data are mean ± SEM ($n = 6$ assays, $^{*}p < 0.05$ compared to the group transfected with ΔCaM)

and DAPK1-KD$^{loxp/loxp}$ mice, but DAPK1-KD$^{-/-}$ aged mice showed better performance in all measured indices than DAPK1-KD$^{loxp/loxp}$ aged mice. Meanwhile, we conducted a contextual fear condition test to analyze hippocampus-dependent learning and memory. Our results showed that DAPK1-KD$^{-/-}$ aged mice significantly improved trace learning, as demonstrated by the increased percentage of freezing time in the context (54.52 ± 7.47% in DAPK1-KD$^{-/-}$ aged mice versus 30.93 ± 2.96% in DAPK1-KD$^{loxp/loxp}$ aged mice) (Fig. 5g), but no tone difference was observed among these groups (Fig. 5h). Most importantly, these data reveal that genetic deletion of the DAPK1 kinase domain in the hippocampus may rescue learning and memory deficits in aging mice.

Discussion

Cognitive dysfunction has become one of the most detrimental threats to health worldwide, among which age-related cognitive decline is an inevitable phenomenon that severely lowers the quality of life [5]. In terms of the mechanisms of age-related cognitive decline, many studies have focused on the structure of the hippocampus, in consideration of its vulnerability to aging and its critical role in learning and memory [5, 21, 22]. And the majority of these studies have reported that dentate gyrus region of the hippocampus is the most seriously disrupted area [23, 24]. Moreover, recent studies have shown no distinguished loss

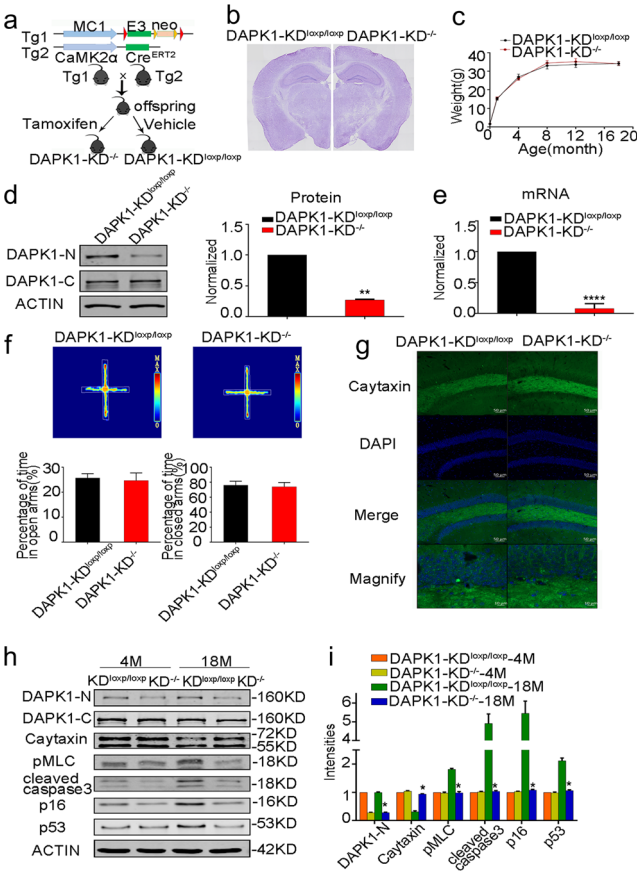

Fig. 4 Inactivation of DAPK1 increases Caytaxin protein. **a** Diagram shows the mouse model of genetic deletion of the kinase domain of DAPK1 specifically in excitatory neurons. **b** Representative images show the hematoxylin staining of the coronal brain sections of DAPK1 knockout and control mice. **c** Graph shows the body weight of DAPK1 knockout and control group in different age groups. Data are mean ± SEM ($n = 15$ assays). **d** Representatives of western blots in cell lysates from the hippocampus of DAPK1 knockout and control mice and bar graph shows the band intensities that were normalized to the respective control (defined as 1.0). Data are mean ± SEM ($n = 6$ assays, $^*p < 0.05$, compared to the respective controls). **e** Bar graph shows the relative expression of mRNA in DAPK1 knockout and control mice. Data are mean ± SEM ($n = 6$ assays, $^{****}p < 0.0001$, compared to the respective controls). **f** Representative images (upper) show the elevated plus maze test of DAPK1 knockout and control mice. Bar graphs (lower) show the percentage of time in open arms (left) and closed arms (right) of DAPK1 knockout and control mice, respectively. Data are mean ± SEM ($n = 15$ assays). **g** Representative images show the expression of Caytaxin in DG region of DAPK1 knockout and control mice. **h** Representatives of western blots in cell lysates from the hippocampus of DAPK1 knockout and control mice at 4 and 18 months. **i** Bar graphs show the band intensities that were normalized to the respective control (defined as 1.0). Data are mean ± SEM ($n = 6$ assays, $^*p < 0.05$, compared to the control group at 18 months)

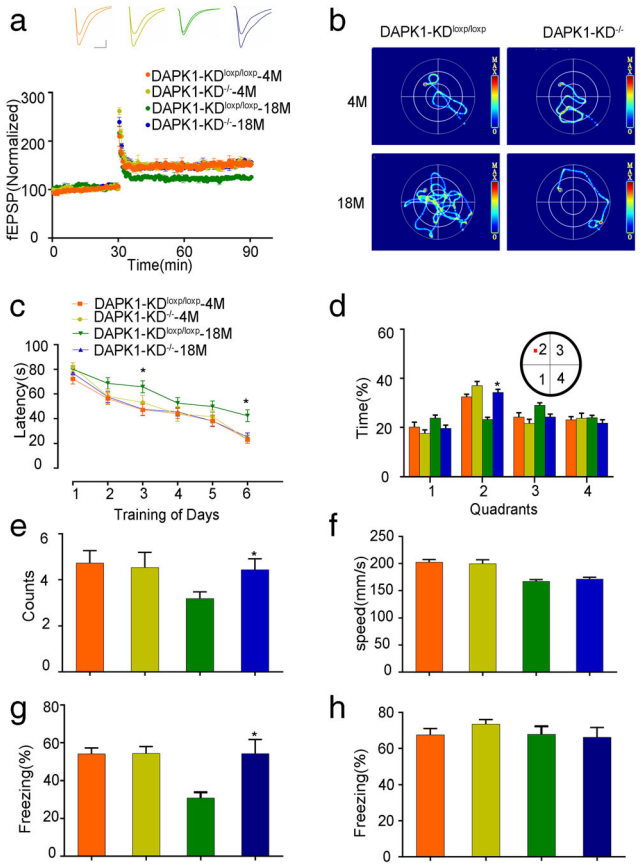

Fig. 5 Inactivation of DAPK1 rescue learning and memory deficits in aging. **a** fEPSPs were recorded in the hippocampus CA1 area from DAPK1 knockout and control mice at 4 and 18 months. The representative recordings (top) and the normalized slope (bottom) of the fEPSPs. **b**–**f** The behaviors of DAPK1 knockout and control mice at 4 and 18 months were examined. **b** Schematic trajectory during the probe trial. **c** The average latency to reach a hidden platform is plotted against the blocks of trials (days) in Morris water maze tests. Data are reported as the mean ± SEM ($n = 15$ mice per group, $^*p < 0.05$, compared to the control group at 18 months). **d** The percentage of time spent in searching of a hidden platform in each quadrant during the probe trial. Data are reported as the mean ± SEM ($n = 15$ mice per group, $^*p < 0.05$, compared to the control group at 18 months). **e** Bar graph shows the times of crossing the place of the hidden platform during the probe trial. Data are reported as the mean ± SEM ($n = 15$ mice per group, $^*p < 0.05$, compared to the control group at 18 months). **f** Bar graph shows the swimming speed of mice during the probe trial. Data are reported as the mean ± SEM ($n = 15$ mice per group). **g**, **h** Bar graphs show the percentage time of freezing during context test (**g**) and tone test (**h**). Data are mean ± SEM ($n = 15$ mice per group, $^*p < 0.05$, compared to the control group at 18 months)

of neurons and no significant expression change of synaptophysin, synaptotagmin, and SNAP25 in the normal aging hippocampus [22, 25, 26]. According to the previous research [27], age-related memory deficit correlates with the changes of neurotransmitter release and synaptic function, rather than loss of neurons or synapses. In this study, we have proved that DAPK1 degrades Caytaxin via activation of capsase3 which impairs learning and memory of the hippocampus in aging mice. Furthermore, genetic deletion of DAPK1 kinase domain in excitatory neurons normalizes the expression of Caytaxin in aging hippocampus and improves learning and memory. Therefore, DAPK1 and Caytaxin may be considered as novel targets for improving aging-related cognitive decline.

Previous studies revealed that DAPK1 was predominantly expressed in the brain. For example, *DAPK1* mRNA had already appeared at embryonic day 13 (E13) and was detected throughout the entire embryonic period. High levels of expression were detected in proliferative and postmitotic neurons within the cerebral cortex and hippocampus. In addition, the overall expression of *DAPK1* mRNA in the brain gradually declined at postnatal stages, and the expression became restricted to hippocampal neurons, in which different expression patterns were observed among rostral, central, and caudal coronal sections, suggesting that DAPK1 may be implicated in neuronal functions of hippocampus [28]. The overall expression of DAPK1 in the brain decreased markedly after birth and the expression was maintained at substantial levels in several restricted mature neuronal populations, such as the olfactory bulb, hippocampus, and granule cells. Its wide expression during development and its maintained expression in the restricted mature neuronal population suggest that DAPK1 might be involved in some neuronal functions beyond simply executing the developmental neuronal cell death [29]. Based on our recent research in Alzheimer's disease, DAPK1 is activated in ECIIPN and knockout of DAPK1 catalytic domain rescues ECIIPN-CA1PV synaptic loss and improves spatial learning and memory in AD mice [30]. Although differences exist between a normal aging and Alzheimer's damaged brain [31, 32], our results depict an upregulation of DAPK1 activity along age-related cognitive decline, but significant improvement in learning and memory in DAPK1 kinase domain knockout mice. Equally, we have shown a decline of Caytaxin expression along with increased DAPK1 activity, and this suppression of Caytaxin expression was found noxious to learning and memory, indicating the role of Caytaxin for DAPK1 activity modulation.

Caytaxin is mainly expressed in the nervous system, specifically in the hilus of dentate gyrus as well as in the cerebellum of Cayman ataxia [33]. It has been demonstrated that Caytaxin is associated with biological functions of cell apoptosis [34, 35], cell migration [36], intracellular transport, and cell differentiation [35]. Immunofluorescence studies further showed the colocalization of Caytaxin and glutaminase with the neuron-specific marker neurofilament-160 at the axon terminals, the neuropil, and synapses of CA3 neurons. These results together support the conclusion that Caytaxin could play an important role in the hippocampus, possibly in the process of neurotransmission at synapses [35]. Our study has indicated a magnificent change in the Caytaxin distribution along the fibers from DG to CA3. Given that Caytaxin is mainly distributed in the fiber of DAPK1-KD$^{-/-}$ mice while having fragmental distribution in DAPK1-KD$^{loxp/loxp}$ mice, we deem that Caytaxin is not only involved in the glutamic acid synthesis, but also in its release and transportation. As to glutamic acid, it works as a main excitatory transmitter for learning and memory [37]. Consistently, Brodsky [38] reported that glutamic acid enhances the weakened communication between neuronal cells during aging. Moreover, our results provide evidence for the interaction of Caytaxin with ZnT3. The zinc ion is a main structural component of many proteins, acting as a cofactor for enzymes critical toward the normal brain functions [39]. The zinc ion, predicted to modulate neuronal excitability, is widely spread in the nervous system especially in the forebrain region including the hippocampus, amygdala, and neocortex [40]. In the hippocampus such as the dentate gyrus, glucoside-rich neurons are abundant in granular cells, mossy fiber, and CA3 as well as CA1 neurons [40]. The zinc-containing fibers from the hippocampus dominate many areas, such as the cerebral cortex, striatum, and marginal areas [41]. Therefore, we consider that Caytaxin regulates learning and memory by regulating glutamic acid.

To clarify whether the aging processes would result in any cross-cellular change in expressions of DAPK1 and Caytaxin, we checked the expression patterns of DAPK1 and Caytaxin in the aging (18 months) mouse brain respectively. By using classic glia cell markers (Iba-1 for microglia, and GFAP for astrocytes), we performed double immunofluorescent staining, and our results showed that neither DAPK1 and Caytaxin co-localize in microglia nor co-exist in astrocytes in the aging (18 months) brain (data not shown). These results indicate that the distributions of DAPK1 and Caytaxin are not affected by the "aging effect." The data provided morphological evidences that DAPK1 and Caytaxin co-exist in the neurons of the aging brain and further confirmed our conclusion that DAPK1 impairs learning and memory by regulating Caytaxin in the hippocampal neurons during aging. Another study has been reported that DAPK1 mediates caspase3 activity [42], as has been verified in our previous research whereby inhibition of DAPK1 activity induced by D-galactose results downregulation of activated caspase3 in senesced cells from DAPK1-KD$^{-/-}$ mice. Moreover, similar downregulation of Caytaxin was also observed in the DAPK1-KD$^{-/-}$ mice. The reduced Caytaxin in the hippocampus at the protein level, but not mRNA, indicates that post-translational regulation of Caytaxin might not be excluded. Either reversible events (such as phosphorylation or sequestration) or irreversible events (proteolysis) could influence the protein levels of Caytaxin. As for this issue, we will investigate further in the following studies.

In conclusion, this study presents that a decrease of Caytaxin due to senescence or Caytaxin suppression using lentivirus can cause learning and memory deficits in mice, while genetic deletion of DAPK1 kinase domain improves the impairment. Coherently, inhibition of DAPK1 or caspase3 activity in vitro reduces Caytaxin degradation. In summary, DAPK1 impairs learning and memory by activating caspase3 to degrade Caytaxin during aging. DAPK1 and Caytaxin are potential targets for the treatment of aging-related cognitive impairment.

Author Contributions YL and LP conceived and designed the studies and wrote the paper. YG and HL carried out the experiments including western blot, qPCR, and mutagenesis and virus construction and behavioral studies. XK and MD performed electrophysiological studies and immunohistochemistry. YC, ZW, HKA, and XZ performed the experiments including genotyping, PCR, and animal breeding. All authors contributed to the data analysis and presentation in the paper.

Funding Information This project was supported by the National Natural Science Foundation of China (Grant No. 31721002 to YL; 91632306 to YL; 51627807 to YL; 81571078 to LP) and the Medjaden Academy & Research Foundation for Young Scientists (Grant No. MJR20160057).

Compliance with Ethical Standards

All mice used in this study were bred and reared in the same conditions in accordance with institutional guidelines of the Animal Care and Use Committee (Huazhong University of Science and Technology, Wuhan, China) within the University' s animal care facility.

Conflict of Interest The authors declare that they have no conflict of interest.

Abbreviations DAPK1, death-associated protein kinase 1; D-GAL, D-galactose; LTP, long-term potentiation; LV, lentivirus; mEPSC, miniature excitatory post synaptic current

References

1. Kowald A (2002) Lifespan does not measure ageing. Biogerontology 3(3):187–190
2. Campos PB, Paulsen BS, Rehen SK (2014) Accelerating neuronal aging in in vitro model brain disorders: a focus on reactive oxygen species. Front Aging Neurosci 6:292. https://doi.org/10.3389/fnagi.2014.00292
3. Harman D (1998) Aging: phenomena and theories. Ann N Y Acad Sci 854:1–7
4. Nyberg L, Lovden M, Riklund K, Lindenberger U, Backman L (2012) Memory aging and brain maintenance. Trends Cogn Sci 16(5):292–305. https://doi.org/10.1016/j.tics.2012.04.005
5. Konar A, Singh P, Thakur MK (2016) Age-associated cognitive decline: insights into molecular switches and recovery avenues. Aging and Disease 7(2):121–129. https://doi.org/10.14336/AD.2015.1004
6. Lustig C, Shah P, Seidler R, Reuter-Lorenz PA (2009) Aging, training, and the brain: a review and future directions. Neuropsychol Rev 19(4):504–522. https://doi.org/10.1007/s11065-009-9119-9
7. Childs BG, Durik M, Baker DJ, van Deursen JM (2015) Cellular senescence in aging and age-related disease: from mechanisms to therapy. Nat Med 21(12):1424–1435. https://doi.org/10.1038/nm.4000
8. Chinta SJ, Woods G, Rane A, Demaria M, Campisi J, Andersen JK (2015) Cellular senescence and the aging brain. Exp Gerontol 68:3–7. https://doi.org/10.1016/j.exger.2014.09.018
9. Bomar JM, Benke PJ, Slattery EL, Puttagunta R, Taylor LP, Seong E, Nystuen A, Chen W et al (2003) Mutations in a novel gene encoding a CRAL-TRIO domain cause human Cayman ataxia and ataxia/dystonia in the jittery mouse. Nat Genet 35(3):264–269. https://doi.org/10.1038/ng1255
10. LeDoux MS (2011) Animal models of dystonia: lessons from a mutant rat. Neurobiol Dis 42(2):152–161. https://doi.org/10.1016/j.nbd.2010.11.006
11. Xiao J, Gong S, Ledoux MS (2007) Caytaxin deficiency disrupts signaling pathways in cerebellar cortex. Neuroscience 144(2):439–461. https://doi.org/10.1016/j.neuroscience.2006.09.042
12. Hayakawa Y, Itoh M, Yamada A, Mitsuda T, Nakagawa T (2007) Expression and localization of Cayman ataxia-related protein, Caytaxin, is regulated in a developmental- and spatial-dependent manner. Brain Res 1129(1):100–109. https://doi.org/10.1016/j.brainres.2006.10.068
13. Bialik S, Kimchi A (2006) The death-associated protein kinases: structure, function, and beyond. Annu Rev Biochem 75:189–210. https://doi.org/10.1146/annurev.biochem.75.103004.142615
14. Tu W, Xu X, Peng L, Zhong X, Zhang W, Soundarapandian MM, Balel C, Wang M et al (2010) DAPK1 interaction with NMDA receptor NR2B subunits mediates brain damage in stroke. Cell 140(2):222–234. https://doi.org/10.1016/j.cell.2009.12.055
15. Cohen O, Inbal B, Kissil JL, Raveh T, Berissi H, Spivak-Kroizaman T, Feinstein E, Kimchi A (1999) DAP-kinase participates in TNF-alpha- and Fas-induced apoptosis and its function requires the death domain. J Cell Biol 146(1):141–148
16. Jin Y, Gallagher PJ (2003) Antisense depletion of death-associated protein kinase promotes apoptosis. J Biol Chem 278(51):51587–51593. https://doi.org/10.1074/jbc.M309165200
17. Raveh T, Droguett G, Horwitz MS, DePinho RA, Kimchi A (2001) DAP kinase activates a p19ARF/p53-mediated apoptotic checkpoint to suppress oncogenic transformation. Nat Cell Biol 3(1):1–7. https://doi.org/10.1038/35050500
18. Parameshwaran K, Irwin MH, Steliou K, Pinkert CA (2010) D-galactose effectiveness in modeling aging and therapeutic antioxidant treatment in mice. Rejuvenation Res 13(6):729–735. https://doi.org/10.1089/rej.2010.1020
19. Carlson DA, Franke AS, Weitzel DH, Speer BL, Hughes PF, Hagerty L, Fortner CN, Veal JM et al (2013) Fluorescence linked enzyme chemoproteomic strategy for discovery of a potent and selective DAPK1 and ZIPK inhibitor. ACS Chem Biol 8(12):2715–2723. https://doi.org/10.1021/cb400407c
20. Itoh M, Li S, Ohta K, Yamada A, Hayakawa-Yano Y, Ueda M, Hida Y, Suzuki Y et al (2011) Cayman ataxia-related protein is a presynapse-specific caspase-3 substrate. Neurochem Res 36(7):1304–1313. https://doi.org/10.1007/s11064-011-0430-5
21. Bettio LEB, Rajendran L, Gil-Mohapel J (2017) The effects of aging in the hippocampus and cognitive decline. Neurosci Biobehav Rev 79:66–86. https://doi.org/10.1016/j.neubiorev.2017.04.030
22. Bishop NA, Lu T, Yankner BA (2010) Neural mechanisms of ageing and cognitive decline. Nature 464(7288):529–535. https://doi.org/10.1038/nature08983
23. Morrison JH, Hof PR (2002) Selective vulnerability of corticocortical and hippocampal circuits in aging and Alzheimer's disease. Prog Brain Res 136:467–486
24. Geinisman Y, Detoledo-Morrell L, Morrell F, Heller RE (1995) Hippocampal markers of age-related memory dysfunction: behavioral, electrophysiological and morphological perspectives. Prog Neurobiol 45(3):223–252. https://doi.org/10.1016/0301-0082(94)00047-l
25. Geinisman Y, Ganeshina O, Yoshida R, Berry RW, Disterhoft JF, Gallagher M (2004) Aging, spatial learning, and total synapse number in the rat CA1 stratum radiatum. Neurobiol Aging 25(3):407–416. https://doi.org/10.1016/j.neurobiolaging.2003.12.001
26. Flood DG, Coleman PD (1988) Neuron numbers and sizes in aging brain: comparisons of human, monkey, and rodent data. Neurobiol Aging 9(5–6):453–463
27. Price JL, Ko AI, Wade MJ, Tsou SK, McKeel DW, Morris JC (2001) Neuron number in the entorhinal cortex and CA1 in preclinical Alzheimer disease. Arch Neurol 58(9):1395–1402

28. Yamamoto M, Takahashi H, Nakamura T (1999) Developmental changes in distribution of death-associated protein kinase mRNAs. J Neurosci Res 5(58):674–683
29. Sakagami H, Kondo H (1997) Molecular cloning and developmental expression of a rat homologue of death-associated protein kinase in the nervous system. Mol Brain Res 2(52):249–256
30. Shu S, Zhu H, Tang N, Chen W, Li X, Li H, Pei L, Liu D et al (2016) Selective degeneration of entorhinal-CA1 synapses in Alzheimer's disease via activation of DAPK1. J Neurosci Off J Soc Neurosci 36(42):10843–10852. https://doi.org/10.1523/JNEUROSCI.2258-16.2016
31. Wyss-Coray T (2016) Ageing, neurodegeneration and brain rejuvenation. Nature 539(7628):180–186. https://doi.org/10.1038/nature20411
32. West MJ, Coleman PD, Flood DG, Troncoso JC (1994) Differences in the pattern of hippocampal neuronal loss in normal ageing and Alzheimer's disease. Lancet 344(8925):769–772
33. Sikora KM, Nosavanh LM, Kantheti P, Burmeister M, Hortsch M (2012) Expression of Caytaxin protein in Cayman Ataxia mouse models correlates with phenotype severity. PLoS One 7(11): e50570. https://doi.org/10.1371/journal.pone.0050570
34. Buschdorf JP, Chew LL, Soh UJ, Liou YC, Low BC (2008) Nerve growth factor stimulates interaction of Cayman ataxia protein BNIP-H/Caytaxin with peptidyl-prolyl isomerase Pin1 in differentiating neurons. PLoS One 3(7):e2686. https://doi.org/10.1371/journal.pone.0002686
35. Buschdorf JP, Li Chew L, Zhang B, Cao Q, Liang FY, Liou YC, Zhou YT, Low BC (2006) Brain-specific BNIP-2-homology protein Caytaxin relocalises glutaminase to neurite terminals and reduces glutamate levels. J Cell Sci 119(Pt 16):3337–3350. https://doi.org/10.1242/jcs.03061
36. Kang JS, Bae GU, Yi MJ, Yang YJ, Oh JE, Takaesu G, Zhou YT, Low BC et al (2008) A Cdo-Bnip-2-Cdc42 signaling pathway regulates p38alpha/beta MAPK activity and myogenic differentiation. J Cell Biol 182(3):497–507. https://doi.org/10.1083/jcb.200801119
37. McEntee WJ, Crook TH (1993) Glutamate: its role in learning, memory, and the aging brain. Psychopharmacology 111(4):391–401
38. Brodsky VY, Malchenko LA, Butorina NN, Lazarev Konchenko DS, Zvezdina ND, Dubovaya TK (2017) Glutamic acid as enhancer of protein synthesis kinetics in hepatocytes from old rats. Biochemistry Biokhimiia 82(8):957–961. https://doi.org/10.1134/S0006297917080119
39. Paoletti P, Vergnano AM, Barbour B, Casado M (2009) Zinc at glutamatergic synapses. Neuroscience 158(1):126–136. https://doi.org/10.1016/j.neuroscience.2008.01.061
40. Gower-Winter SD, Levenson CW (2012) Zinc in the central nervous system: from molecules to behavior. BioFactors 38(3):186–193. https://doi.org/10.1002/biof.1012
41. Szewczyk B (2013) Zinc homeostasis and neurodegenerative disorders. Front Aging Neurosci 5:33. https://doi.org/10.3389/fnagi.2013.00033
42. Bialik S, Kimchi A (2014) The DAP-kinase interactome. Apoptosis: an international journal on programmed cell death 19(2):316–328. https://doi.org/10.1007/s10495-013-0926-3